



BRIEF COMMUNICATION

A recurrent, homozygous *EMC10* frameshift variant is associated with a syndrome of developmental delay with variable seizures and dysmorphic features

Diane D. Shao^{1,2}, Rachel Straussberg^{3,4,24}, Hind Ahmed^{5,24}, Amjad Khan⁵, Songhai Tian⁶, R. Sean Hill^{2,7}, Richard S. Smith², Amar J. Majmudar⁸, Najim Ameziane⁹, Jennifer E. Neil^{2,7}, Edward Yang¹⁰, Amal Al Tenaiji¹¹, Saumya S. Jamuar^{12,13}, Thorsten M. Schlaeger¹⁴, Muna Al-Saffar^{2,15}, Iris Hovel⁹, Aisha Al-Shamsi¹⁶, Lina Basel-Salmon^{4,17}, Achiya Z. Amir^{4,18}, Lariza M. Rento^{2,7}, Jiin Ying Lim^{12,13}, Indra Ganesan¹², Shirlee Shril⁸, Gilad Evrony^{2,19}, A. James Barkovich²⁰, Peter Bauer⁹, Friedhelm Hildebrandt⁸, Min Dong⁶, Guntram Borck^{21,23}, Christian Beetz^{9,25}, Lihadh Al-Gazali^{22,25}, Wafaa Eyaid^{5,25} and Christopher A. Walsh^{2,7,25}✉

PURPOSE: The endoplasmic reticulum membrane complex (EMC) is a highly conserved, multifunctional 10-protein complex related to membrane protein biology. In seven families, we identified 13 individuals with highly overlapping phenotypes who harbor a single identical homozygous frameshift variant in *EMC10*.

METHODS: Using exome, genome, and Sanger sequencing, a recurrent frameshift *EMC10* variant was identified in affected individuals in an international cohort of consanguineous families. Multiple families were independently identified and connected via Matchmaker Exchange and internal databases. We assessed the effect of the frameshift variant on *EMC10* RNA and protein expression and evaluated *EMC10* expression in normal human brain tissue using immunohistochemistry.

RESULTS: A homozygous variant *EMC10* c.287delG (Refseq NM_206538.3, p.Gly96Alafs*9) segregated with affected individuals in each family, who exhibited a phenotypic spectrum of intellectual disability (ID) and global developmental delay (GDD), variable seizures and variable dysmorphic features (elongated face, curly hair, cubitus valgus, and arachnodactyly). The variant arose on two founder haplotypes and results in significantly reduced *EMC10* RNA expression and an unstable truncated EMC10 protein.

CONCLUSION: We propose that a homozygous loss-of-function variant in *EMC10* causes a novel syndromic neurodevelopmental phenotype. Remarkably, the recurrent variant is likely the result of a hypermutable site and arose on distinct founder haplotypes.

Genetics in Medicine _#####_; <https://doi.org/10.1038/s41436-021-01097-x>

INTRODUCTION

The endoplasmic reticulum membrane complex (EMC) consists of multiple proteins that are highly conserved across eukaryotes.¹ This complex has been shown to play a critical role as a transmembrane protein insertase, facilitating the proper insertion of some tail-anchored membrane proteins and multipass transmembrane proteins.^{2,3} Of the ten proteins that form the human EMC, only variants in *EMC1* have previously been associated with a genetic syndrome that includes global developmental delay (GDD), cerebellar atrophy, seizures, microcephaly, and vision abnormalities^{4,5} (OMIM 616875).

In this study, we report 13 individuals from seven consanguineous nuclear families who are affected with a syndromic

phenotype including GDD, intellectual disability (ID), variable seizures, and variable dysmorphic features including a long face, curly hair, cubitus valgus, and arachnodactyly. This phenotype segregated with a homozygous *EMC10* frameshift variant that appears to be a mutational hotspot. Using in vitro studies, we provide additional evidence for the deleterious effect of this *EMC10* variant.

MATERIALS AND METHODS

Clinical presentation was assessed by a clinical geneticist from one of the participating clinical centers, and informed consent for publication of individual photos was also obtained. Exome, genome sequencing, and/or single-nucleotide polymorphism

¹Department of Neurology, Boston Children's Hospital, Boston, MA, USA. ²Division of Genetics and Genomics, Department of Pediatrics, Boston Children's Hospital, Boston, MA, USA. ³Neurogenetics Clinic, Neurology Unit, Schneider Children Medical Center, Petah Tikvah, Israel. ⁴Sackler School of Medicine, Tel Aviv University, Ramat Aviv, Israel. ⁵Genetics Division, Department of Pediatrics, King Abdullah International Medical Research Centre, King Saud bin Abdulaziz University for Health Science, King Abdulaziz Medical City, Ministry of National Guard-Health Affairs (NGHA), Riyadh, Saudi Arabia. ⁶Department of Urology, Boston Children's Hospital, and Department of Surgery and Department of Microbiology, Harvard Medical School, Boston, MA, USA. ⁷Howard Hughes Medical Institute, Boston Children's Hospital, Boston, MA, USA. ⁸Division of Nephrology, Department of Pediatrics, Boston Children's Hospital, Boston, MA, USA. ⁹Centogene AG, Rostock, Germany. ¹⁰Department of Radiology, Boston Children's Hospital, Boston, MA, USA. ¹¹Medical Institute of Medical Affairs, Sheikh Khalifa Medica City, Abu Dhabi, UAE. ¹²Department of Pediatrics, KK Women's and Children's Hospital, Ramat Aviv, Israel. ¹³SingHealth Duke-NUS Genomic Medicine Centre, Singapore, Singapore. ¹⁴Stem Cell Program, Boston Children's Hospital, Harvard Medical School, and Harvard Stem Cell Institute, Harvard University, Boston, MA, USA. ¹⁵Department of Pediatrics, United Arab Emirates University, Abu Dhabi, UAE. ¹⁶Division of Genetics, Department of Pediatrics, Tawam Hospital, Al Ain, UAE. ¹⁷Raphael Recanati Genetic Institute, Rabin Medical Center–Beilinson Hospital and Pediatric Genetics Clinic, Schneider Children's Medical Center, and Felsenstein Medical Research Center, Petah Tikvah, Israel. ¹⁸Pediatric Gastroenterology, Hepatology and Nutrition Clinic, Dana-Dwek Children's Hospital, Tel Aviv Medical Center, Ramat Aviv, Israel. ¹⁹New York University School of Medicine, Center for Human Genetics & Genomics, New York, NY, USA. ²⁰Neuroradiology, University of California at San Francisco, San Francisco, CA, USA. ²¹Center for Rare Diseases (ZSE Ulm), Ulm University Medical Center, Ulm, Germany. ²²Department of Pediatrics, United Arab Emirates University, Al Ain, UAE. ²³Present address: genetikum, Neu-Ulm, Germany. ²⁴These authors contributed equally: Rachel Straussberg, Hind Ahmed. ²⁵These authors contributed equally: Christian Beetz, Lihadh Al-Gazali, Wafaa Eyaid, Christopher A. Walsh. ✉email: Christopher.Walsh@childrens.harvard.edu

(SNP) array, were performed either through clinical diagnostic testing at Centogene and/or through research settings. See Supplemental Material for institution-specific gene discovery methods. Collaborators were connected via Matchmaker Exchange⁶ and existing scientific networks. Genome-wide linkage analysis was performed to generate a logarithm of the odds (LOD) score from SNP array data using Merlin under a recessive mode of inheritance assuming a disease allele prevalence of 0.0001 and full penetrance. Haplotype analysis from exome and genome sequencing data considered only variants in regions that are covered by both genome and exome sequencing. A 2-Mb region up and downstream of the relevant *EMC10* variant was interrogated (chr19: 48981900–52961200 [hg19]) and filtered for high quality homozygous variants.

Further details of genetic and experimental methods can be found in Supplemental Material.

RESULTS

Genetic findings

Using exome or genome sequencing, we identified a biallelic *EMC10* frameshift variant at RefSeq NM_206538.3: c.287delG (p. Gly96Alafs*9), in all affected individuals with shared phenotype in seven consanguineous families of Bedouin, Saudi Arabia, and United Arab Emirates origin (Fig. 1a). None of the individuals had other rare variants predicted to alter gene function in any previously reported genes associated with neurodevelopmental conditions. There are no individuals who are homozygous for the *EMC10* c.287delG variant in human reference databases such as gnomAD,⁷ GenomeAsia 100K Project,⁸ and the Greater Middle East Variome.⁹ No individuals with biallelic loss-of-function variants in

EMC10 were identified by comprehensively searching Centogene's disease-associated variant database CentoMD,¹⁰ which contains data from >80,000 individuals with hereditary disorders analyzed by exome or genome sequencing. Sanger sequencing confirmed segregation of the *EMC10* variant with disease in all families, including the extended family tree of affected individuals in families 1 and 2 (Fig. S1).

Genome-wide linkage analysis to the phenotype of intellectual disability determined a maximum LOD score of 6.49 on chromosome 19, consistent with the location of *EMC10* (Fig. 1b). There were no other genomic regions that exhibited significant linkage. Linkage analysis using only array data for affected individuals (thus removing the assumption that siblings, who were not directly assessed, are truly unaffected) showed linkage to the same region. Regions of homozygosity (ROH) were also reviewed from SNP array, exome, or genome sequencing data, and ranged from 1.1 Mb to 2.8 Mb. The consensus ROH was ~225 kB in size (hg19 chr19: 50789967–51015404), in which the only shared coding variant was in *EMC10* (Fig. 1c).

Because the variant was identical in multiple unrelated families, we looked specifically at whether there was a founder effect (i.e., a single shared haplotype) or a potential hotspot for genetic variation (i.e., a variant that arose in multiple haplotypes). Haplotype analysis clearly showed two distinct haplotypes based on SNPs from exome sequencing (Fig. 1d). SNP array data also supported the presence of two distinct haplotypes, and included family 6 for whom exome data was unavailable (Fig. S2). Haplotypes were shared by affected individuals of families 1 and 2 who are second cousins, and a separate haplotype was identified in families 3 through 7.

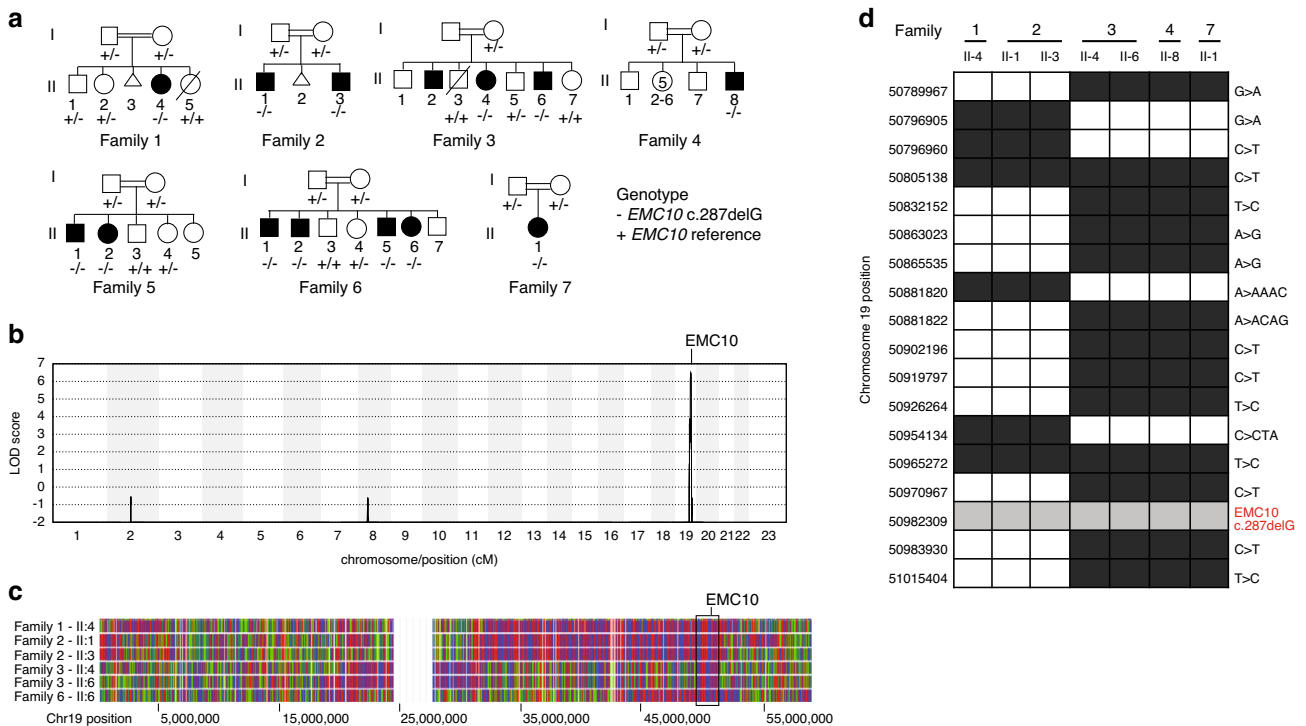


Fig. 1 *EMC10* variant segregates with disease phenotype in multiple affected families. (a) Pedigrees of affected families. Affected individuals in families 1 and 2 are second cousins. Affected individuals in families 5 and 6 are first cousins. Solid black, affected. Genotypes, where indicated, represent results of evaluation for the *EMC10* c.287delG variant by Sanger sequencing. (b) Genome-wide logarithm of the odds (LOD) score distribution. (c) Affected individuals share a region of homozygosity on chromosome 19 (boxed), overlapping the location of *EMC10* variant. Single-nucleotide polymorphism (SNP) array data for affected individuals in families 1, 2, 3, and 6 are shown. Homozygous SNPs are displayed in red or blue. Heterozygous SNPs are displayed in green. (d) Haplotypes based on SNPs determined from sequencing data in the consensus region of homozygosity (chr19: 50789967–51015404) indicate that *EMC10* variant arose on two distinct haplotypes. SNP array independently confirmed two haplotypes (Fig. S2).

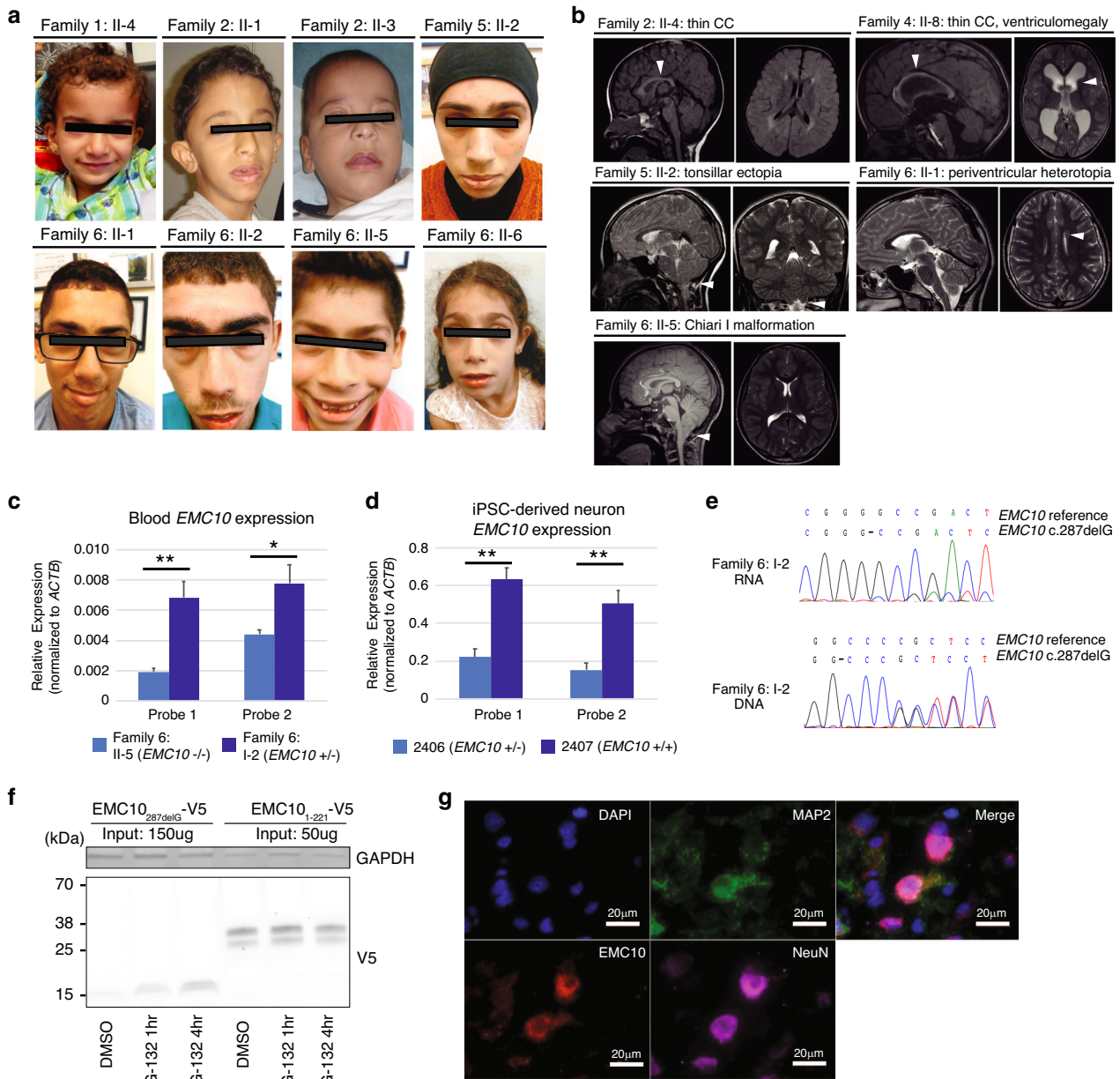


Fig. 2 Clinical features of affected individuals. **(a)** Facial appearance of affected individuals. **(b)** Representative brain abnormalities on magnetic resonance image (MRI). See Table S2 for summary of imaging findings. **(c)** *EMC10* RNA expression relative to *ACTB* in blood from affected individual and unaffected parent. Single-sided *t*-test $*p < 0.01$, $**p < 0.005$. **(d)** *EMC10* RNA expression relative to *ACTB* in induced pluripotent stem cells (iPSC)-derived neurons from individual heterozygous for *EMC10* variant, and related individual without the variant. Both individuals are relatives of family 2 (pedigree in Fig. S1). Single-sided *t*-test $**p < 0.005$. **(e)** Sanger sequencing traces from DNA and RNA (complementary DNA [cDNA]) from an individual heterozygous for the reported *EMC10* variant. The DNA sequencing trace is displayed as reverse complement. **(f)** Proteasome inhibition by MG-132 rescues expression of V5-tagged truncated *EMC10*_{287delG} in a time-dependent manner. **(g)** *EMC10* protein (red) is observed primarily in neurons in primary tissue from human brain. Neurons are marked by nuclear membrane staining for NeuN (magenta) or non-nuclear staining for MAP2 (green). *EMC10* colocalizes with neuronal markers MAP2 and NeuN.

Clinical characteristics

Clinical findings for all 13 affected individuals show a core phenotype of GDD/ID and, to a lesser extent, dysmorphic features and seizures (Table S1). Facial dysmorphisms described in multiple individuals include a long face, pointed chin, and curly hair, although evaluation by several dysmorphologists did not concur on a consistent facial gestalt (Fig. 2a). Limb anomalies included cubitus valgus (6/13), arachnodactyly (3/13), and bilateral 5th digit clinodactyly (1/13). Most individuals exhibited GDD in domains including social, motor, language, and cognitive, and/or ID (11/12). Individual II-1 in family 7 was age 3 months at ascertainment; thus

most milestones could not be assessed. Seizures were noted in 6/13 individuals, typically during childhood or in the neonatal period, and included multifocal as well as generalized tonic-clonic seizures. The majority of affected individuals who underwent brain magnetic resonance imaging (MRI) had abnormal findings (9/10); however, findings were individually nonspecific, including cerebellar tonsillar ectopia or Chiari I (4/12), a thin corpus callosum (3/10), and white matter signal abnormalities (3/10) (Fig. 2b; Table S2). Neurologic symptoms appeared to be static or nonprogressive.

Additional minor features included failure to thrive (4/13), umbilical and inguinal hernias (5/13), and ventricular septal

defects (2/13). Renal abnormalities of any kind were present in 9/13 affected individuals (69%) (Fig. S3; Table S3). There is no correspondence of renal phenotype to the two haplotypes at the *EMC10* locus. Renal abnormalities included nephrocalcinosis (4/11), mild hydronephrosis or hydroureter (2/11), and renal cysts (3/11; unilateral cyst in 2 individuals, bilateral cysts in 1 individual). One individual had end-stage renal disease of unclear etiology, which required kidney transplantation. The variability in renal phenotype was suggestive of different underlying genetic mechanisms, and less likely to be attributed specifically to the *EMC10* variant. Multiple liver cystic lesions were incidentally identified individual II-6 from family 6 (Fig. S4).

EMC10 functional assessment of variant and expression in human brain tissue

The *EMC10* c.287delG frameshift variant is expected to result in nonsense-mediated messenger RNA (mRNA) decay. *EMC10* expression is significantly reduced, but not absent, in affected individuals as determined by evaluation of RNA expression from blood by droplet digital polymerase chain reaction (PCR) in family 6: II-5 and his unaffected mother I-2, who is heterozygous for the *EMC10* variant (Fig. 2c). For each sample described, a negative control reaction performed without reverse transcriptase confirmed that there was no DNA contamination in the extracted RNA. Furthermore, in neurons derived from induced pluripotent stem cells from relatives of families 1 and 2 (individuals 2406 and 2407 indicated in Fig. S1; Fig. 2d), *EMC10* expression is reduced in heterozygotes compared with individuals without the variant. Finally, we amplified *EMC10* complementary DNA (cDNA) in family 6: I-2 (*EMC10* +/−) using PCR, and showed that Sanger sequencing traces confirmed allelic imbalance, with decreased abundance of RNA transcripts that harbor the single-nucleotide deletion (Fig. 2e).

Although a small fraction of RNA that includes the *EMC10* frameshift variant is expressed, we show that this transcript results in an unstable protein. The potential truncated protein is 103 amino acids in length. The last 8 amino acids are altered due to frameshift and disrupts a region of high amino acid conservation (Figs. S5, S6). A signal peptide (amino acids 1–27) is cleaved in the mature form of EMC10 (UniprotKB accession U5QCC4). The C-terminal region, which interacts with core EMC proteins,^{11,12} would be abolished by the truncation. We cloned the open reading frame of *EMC10*, from residue 1 to the terminal residue of p.Gly96Argfs*9, into an expression vector (*EMC10*_{287delG}). We also created another *EMC10* truncation mutant that stops at residue 103 (*EMC10*_{1–103}), which retains the wild-type amino acids but mimics the length of the truncation variant. Finally, we created a truncated 221 residue construct that included the entire luminal domain (*EMC10*_{1–221}), as control for expression of our allele. All constructs were tagged with a V5 epitope for detection and expressed in HeLa cells via transient transfection (Fig. S7). *EMC10*_{1–221} was detected in cells; in contrast, neither *EMC10*_{287delG} nor *EMC10*_{1–103} was detectable in cell lysates, suggesting that these two shorter truncated fragments are unstable. We showed that this instability is due to proteasomal degradation. Cells transfected with the *EMC10*_{287delG} or *EMC10*_{1–221} construct were treated with proteasomal inhibitor MG-132, which rescued protein expression in a time-dependent manner (Fig. 2f).

We assessed expression of endogenous EMC10 in postmortem infant human brain using immunohistochemistry (Fig. 2g). Specificity of the EMC10 antibody was confirmed by immunoblotting for EMC10 after transfection of commercially validated small interfering RNA (siRNA) (Fig. S8). Staining for EMC10 in postmortem human infant brain showed colocalization with MAP2, a non-nuclear protein expressed in mature neurons. NeuN, a nuclear marker of mature neurons, also showed colocalization with EMC10.

DISCUSSION

We describe a syndromic phenotype including GDD/ID, seizures, and variable dysmorphic features and limb abnormalities, associated with autosomal recessive inheritance of a recurrent, loss-of-function frameshift variant in *EMC10*. Our cohort exhibits multiple renal abnormalities, which are difficult to reconcile with a single underlying genetic mechanism; thus, we cannot confidently ascribe a renal phenotype to the reported variant. Intriguingly, all the families identified shared the exact same *EMC10* variant, and we showed that the variant arose independently in two founder haplotypes. The single-nucleotide deletion occurs in a homopolymeric repeat sequence (CGGGGC) that predisposes to DNA replication errors and represents a potential hotspot for genetic variation. In addition, deletion of any one of the four consecutive G residues would create an indistinguishable frameshift allele. Recurrent variants at sites of homopolymeric G/C nucleotides have been identified in several disorders with monoallelic^{13,14} or biallelic¹⁵ inheritance.

Comparison of the *EMC10* phenotype to the published *EMC1* phenotype⁴ shows common features of GDD, present in all families for both diseases (Table S4). Individuals with *EMC10* variants had higher rates of seizures compared to *EMC1*, and individuals with *EMC1* variants had cerebellar or cerebral atrophy that was not seen in the *EMC10* cohort. Abnormalities of the corpus callosum were observed in both cohorts.

Homozygous *EMC10* knockout mice were characterized by the International Mouse Genotyping Consortium¹⁶ (www.mousephenotype.org) and exhibited statistically significant changes on behavioral assessments compared with control mice. Differences include abnormal vocalization, gait, activity, and behavior during open field testing, which measures motor activity and anxiety-related behaviors in rodents (Fig. S9). Another *EMC10* knockout model identified differences in cognitive processes such as working memory and associative emotional learning.¹⁷ Other published murine knockout models did not specifically assess neurobehavioral phenotypes.^{18,19} Further studies are required to understand whether the observed abnormalities in murine models directly reflect the neurocognitive profiles of humans with *EMC10* variants.

Transmembrane proteins have a spontaneous rate of protein membrane insertion, and this rate is enhanced by a functioning EMC.² Changes in EMC function are likely to decrease, but not abolish, the insertion and proper function of multiple transmembrane proteins. Indeed, a survey of 61 proteins dependent upon the EMC in proteomic studies (Tian et al.²⁰ and Shurtleff et al.²¹) revealed that many have been independently implicated in human neurodevelopmental diseases (Table S5). EMC10 is ubiquitously expressed in the body including in the brain, kidney, gastrointestinal tract, and musculoskeletal tissue;²² thus it is not surprising that the disease phenotype also involves multiple organs.

In summary, we implicate *EMC10* as a gene whose disruption leads to a human neurodevelopmental syndrome. The systemic nature of the phenotype highlights the pleiotropic roles of the EMC. Open questions remain in terms of the variability of the phenotype despite a single recurrent variant and the functional role of EMC10 in different organ systems.

DATA AVAILABILITY

De-identified materials, data sets, and protocols are available upon request. The reported variant was submitted to ClinVar: SUB8682021.

Received: 7 August 2020; Revised: 28 December 2020; Accepted: 4 January 2021;

Published online: 02 February 2021

REFERENCES

- Wideman, J. G. The ubiquitous and ancient ER membrane protein complex (EMC): tether or not? *F1000Research*. **4**, 624 (2015).
- Chitwood, P. J., Juszkievicz, S., Guna, A., Shao, S. & Hegde, R. S. EMC is required to initiate accurate membrane protein topogenesis. *Cell*. **175**, 1507–1519.e16 (2018).
- Guna, A., Volkmar, N., Christianson, J. C. & Hegde, R. S. The ER membrane protein complex is a transmembrane domain insertase. *Science*. **359**, 470–473 (2018).
- Harel, T. et al. Monoallelic and biallelic variants in EMC1 identified in individuals with global developmental delay, hypotonia, scoliosis, and cerebellar atrophy. *Am. J. Hum. Genet.* **98**, 562–570 (2016).
- Abu-Safieh, L. et al. Autozygome-guided exome sequencing in retinal dystrophy patients reveals pathogenic mutations and novel candidate disease genes. *Genome Res.* **23**, 236–247 (2013).
- Philippakis, A. A. et al. The Matchmaker Exchange: a platform for rare disease gene discovery. *Hum. Mutat.* **36**, 915–921 (2015).
- Lek, M. et al. Analysis of protein-coding genetic variation in 60,706 humans. *Nature*. **536**, 285–291 (2016).
- The GenomeAsia 100K. Project enables genetic discoveries across Asia. *Nature*. **576**, 106–111 (2019).
- Greater Middle East Variome. <http://igm.ucsd.edu/gme/index.php> (2020).
- Trujillano, D., Oprea, G.-E., Schmitz, Y., Bertoli-Avella, A. M., Abou Jamra, R. & Rolfs, A. A comprehensive global genotype-phenotype database for rare diseases. *Mol. Genet. Genomic Med.* **5**, 66–75 (2017).
- Pleiner, T., Pinton Tomaleri, G., Januszzyk, K., Inglis, A. J., Hazu, M. & Voorhees, R. M. Structural basis for membrane insertion by the human ER membrane protein complex. *Science*. **24**, 433–436 (2020).
- O'Donnell, J. P. et al. The architecture of EMC reveals a path for membrane protein insertion. *Elife*. **9**, e57887 (2020).
- Amiel, J. et al. PAX2 mutations in renal-coloboma syndrome: mutational hotspot and germline mosaicism. *Eur. J. Hum. Genet.* **8** (2000).
- Cortese, A. et al. Biallelic mutations in SORD cause a common and potentially treatable hereditary neuropathy with implications for diabetes. *Nat. Genet.* **52**, 473–481 (2020).
- Ghosh, S. G. et al. Recurrent homozygous damaging mutation in TMX2, encoding a protein disulfide isomerase, in four families with microlissencephaly. *J. Med. Genet.* **57** (2020).
- Dickinson, M. E. et al. High-throughput discovery of novel developmental phenotypes. *Nature*. **537**, 508–514 (2016).
- Diamantopoulou, A. et al. Loss-of-function mutation in Mirta22/Emc10 rescues specific schizophrenia-related phenotypes in a mouse model of the 22q11.2 deletion. *Proc. Natl. Acad. Sci. U. S. A.* **114**, E6127–E6136 (2017).
- Zhou, Y. et al. EMC10 governs male fertility via maintaining sperm ion balance. *J. Mol. Cell. Biol.* **10**, 503–514 (2018).
- Reboll, M. R. et al. EMC10 (Endoplasmic Reticulum Membrane Protein Complex Subunit 10) is a bone marrow-derived angiogenic growth factor promoting tissue repair after myocardial infarction. *Circulation*. **136**, 1809–1823 (2017).
- Tian, S. et al. Proteomic analysis identifies membrane proteins dependent on the ER membrane protein complex. *Cell. Rep.* **28**, 2517–2526.e5 (2019).
- Shurtleff, M. J. et al. The ER membrane protein complex interacts cotranslationally to enable biogenesis of multipass membrane proteins. *Elife*. **7**, e37018 (2018).
- Human Protein Atlas. <http://www.proteinatlas.org> (2020).

ACKNOWLEDGEMENTS

We are sincerely indebted to the generosity of the families and patients who participated in this study. We acknowledge clinicians (names withheld) whose contributions enhanced our understanding of the patient phenotype, but who could not formally participate in this work due to geopolitical conflicts. We acknowledge Connor Kenny, who performed Sanger validation. Human postmortem brain tissue was obtained from the National Institutes of Health (NIH) Neurobiobank at the University of Maryland in Baltimore. We thank the Thomas Sudhof Laboratory at Stanford University for gifting lentiviral vectors for NGN2 transduction to the Human Neuron Core at Boston Children's Hospital (BCH). The Human Neuron Core is supported by BCH IDDC U54HD090255 and played the key role in generation of neurons derived from induced pluripotent stem cells (iPSCs). The Yale Center for Mendelian Genomics (UM1HG006504), funded by the National Human Genome Research Institute, and the GSP Coordinating Center (U24 HG008956) provided sequencing, and logistical and general study coordination, respectively.

AUTHOR CONTRIBUTIONS

Conceptualization: D.D.S., R.S., H.A., C.B., L.A., W.E., C.A.W. Investigation: R.S., H.A., A.K., A.A.T., M.A., A.A., L.B., A.Z.A., S.S.J., J.L., I.G., L.A., W.E. Data curation: D.D.S., A.K., J.E.N., A. J.B. and A.J.M. Validation and methodology: D.D.S., R.S.H., N.A.A., S.T., T.M.S., R.S.S., and L.M.R. Formal analysis: A.J.M., R.S.H., N.A., I.H., G.E., J.A.B., P.B., S.S., A.J.M., F.H., G.B., and C.B. Supervision: F.H., G.B., M.D., C.B., L.A., W.E., C.A.W. Visualization: E.Y. and A.J.B., D.D. S., R.S., N.A., S.T., A.J.M., and J.E.N. Writing—original draft: D.D.S. Writing—reviewing and editing: all authors.

FUNDING

C.A.W. is supported by National Institute of Neurologic Disorders and Stroke (NINDS) (RO1 35129) and is an Investigator of the Howard Hughes Medical Institute. This research was supported by the Allen Discovery Center program, a Paul G. Allen Frontiers Group advised program of the Paul G. Allen family Foundation. D.D.S. is supported by NINDS Neurology Resident Research Education Program (R25 NS070682). R.S.S. is supported by National Institute of Health (NIH) K99NS112604. A.J.M. acknowledges support from NIH Training Grant (T32DK-007726), the 2017 Postdoctoral Fellowship Grant from the Harvard Stem Cell Institute, and the American Society of Nephrology Lipps Research Program 2018 Polycystic Kidney Disease Foundation Jared J. Grantham Research Fellowship. M.D. acknowledges support from NIH (R01NS080833 and R21NS106159), the NIH-funded Harvard Digestive Disease Center (P30DK034854) and BCH Intellectual and Developmental Disabilities Research Center (P30HD18655). M. D. holds the Investigator in the Pathogenesis of Infectious Disease Award from the Burroughs Wellcome Fund. F.H. is the William E. Harmon Professor of Pediatrics and this work was supported by grants from the NIH DK-068306.

ETHICS DECLARATION

Individuals presented herein were identified and evaluated in a clinical setting, and biological samples were collected after obtaining written informed clinical and/or research consent according to protocols approved by their respective institutional review boards (IRBs) (BCH, United Arab Emirates University, Schneider Children's Medical Center, and Prince Sultan Military Medical City). Postmortem human brain tissue was obtained from the University of Maryland Brain and Tissue Bank of the NIH NeuroBioBank obtained according to IRB for the University of Maryland and NIH Neurobiobank policies. Consent was obtained for publication of photographs with exclusion of eyes for de-identification.

COMPETING INTERESTS

N.A., I.H., P.B., and C.B. are current or former employees of Centogene AG, Rostock, Germany. The other authors declare no competing interests.

ADDITIONAL INFORMATION

Supplementary information The online version contains supplementary material available at <https://doi.org/10.1038/s41436-021-01097-x>

Correspondence and requests for materials should be addressed to C.A.W.

Reprints and permission information is available at <http://www.nature.com/reprints>

Publisher's note Springer Nature remains neutral with regard to jurisdictional claims in published maps and institutional affiliations.



Open Access This article is licensed under a Creative Commons Attribution 4.0 International License, which permits use, sharing, adaptation, distribution and reproduction in any medium or format, as long as you give appropriate credit to the original author(s) and the source, provide a link to the Creative Commons license, and indicate if changes were made. The images or other third party material in this article are included in the article's Creative Commons license, unless indicated otherwise in a credit line to the material. If material is not included in the article's Creative Commons license and your intended use is not permitted by statutory regulation or exceeds the permitted use, you will need to obtain permission directly from the copyright holder. To view a copy of this license, visit <http://creativecommons.org/licenses/by/4.0/>.

© The Author(s) 2021